Reduction of Theta Rhythm Dissociates Grid Cell Spatial Periodicity from Directional Tuning

Mark P. Brandon, *et al.*

Science **332**, 595 (2011);
DOI: 10.1126/science.1201652

cy of the hippocampo-entorhinal circuitry (*25*) when pacing by septal inputs was reduced.

Hippocampal place cells are also spatially modulated cells without periodicity in their firing pattern. Their spatial firing patterns are partially affected in the radial maze after septal inactivation and in the open field during reduced cholinergic neurotransmission (*26*, *27*). For comparisons with MEC cells, we therefore recorded from hippocampal place cells in the same experimental design while reducing theta oscillations to the same extent as in MEC recordings (fig. S2) (*20*). We observed a substantial decrease in the firing rate of hippocampal place cells, and the spike trains of individual hippocampal cells showed reduced theta modulation (Fig. 3A and fig. S2). Place fields remained well-defined and at corresponding locations (Fig. 3, B and C, figs. S9 and S10, and table S1).

By silencing the septal area, we diminished theta oscillations in the entorhino-hippocampal circuitry and showed that the periodic firing of grid cells does not persist. Subcortical inputs to hippocampus and parahippocampal cortices are thus essential not only for theta oscillations but also for sustaining the spatial periodicity of grid cells. These findings are consistent with the theory that grid cells emerge from the interference between multiple precisely tuned theta oscillations within individual cells (*12*–*14*). Alternatively, the silencing of septal inputs to the MEC might result in the desynchronization of grid cells, so that the local network of cortical cells can no longer generate oscillatory interference (*12*, *28*). Our data also identified a subpopulation of grid cells that do not regain their spatial regularity when theta oscillations recover (fig. S6). This suggests that a fraction of grid cells might not be directly participating in the generation of grid patterns, but rather becomes associated with other grid cells by plasticity-dependent mechanisms.

A parallel study (*29*) has independently discovered that grid cell firing does not persist during reduced theta oscillations and that other cell types are less affected. Together, our results show that the neuronal network mechanisms that sustain the periodic spatial firing of grid cells are different from those required for other firing correlates in the entorhino-hippocampal circuitry, including head-direction cells and place cells. The effect on grid cells is likely not mediated through effects of septal silencing on the firing of hippocampal place cells, because it has been shown that grid cell firing initially remains intact after the hippocampus has been silenced (*30*). Subcortical inputs are therefore necessary for the neural computations in the MEC that generate grid-like, periodic, spatial firing patterns, whereas the firing locations of place cells largely persist after inputs from grid cells and from subcortical areas to the hippocampus have substantially changed.

References and Notes

1. C. M. Gray, P. König, A. K. Engel, W. Singer, *Nature* **338**, 334 (1989).
2. L. L. Colgin *et al.*, *Nature* **462**, 353 (2009).
3. A. D. Ekstrom *et al.*, *Hippocampus* **15**, 881 (2005).
4. W. Klimesch, *Brain Res. Brain Res. Rev.* **29**, 169 (1999).
5. R. I. Wilson, G. Laurent, *J. Neurosci.* **25**, 9069 (2005).
6. J. O'Keefe, L. Nadel, *The Hippocampus as a Cognitive Map* (Oxford Univ. Press, Oxford, 1978).
7. J. O'Keefe, J. Dostrovsky, *Brain Res.* **34**, 171 (1971).
8. T. Hafting, M. Fyhn, S. Molden, M. B. Moser, E. I. Moser, *Nature* **436**, 801 (2005).
9. J. S. Taube, R. U. Muller, J. B. Ranck Jr., *J. Neurosci.* **10**, 420 (1990).
10. C. N. Boccara *et al.*, *Nat. Neurosci.* **13**, 987 (2010).
11. C. H. Vanderwolf, *Electroencephalogr. Clin. Neurophysiol.* **26**, 407 (1969).
12. N. Burgess, C. Barry, J. O'Keefe, *Hippocampus* **17**, 801 (2007).
13. M. E. Hasselmo, L. M. Giocomo, E. A. Zilli, *Hippocampus* **17**, 1252 (2007).
14. J. O'Keefe, N. Burgess, *Hippocampus* **15**, 853 (2005).
15. H. Petsche, C. Stumpf, G. Gogolak, *Electroencephalogr. Clin. Neurophysiol.* **14**, 202 (1962).
16. S. J. Mizumori, C. A. Barnes, B. L. McNaughton, *Brain Res.* **500**, 99 (1989).
17. R. M. Yoder, K. C. Pang, *Hippocampus* **15**, 381 (2005).
18. K. J. Jeffery, J. G. Donnett, J. O'Keefe, *Neuroreport* **6**, 2166 (1995).
19. Materials and methods are available as supporting material on *Science* Online.
20. Hippocampal and MEC cells were recorded in separate experiments (except for the data in fig. S10). In the MEC, grid cells (n = 26) and other cell types (n = 27 simultanously with grid cells, and n = 37 without grid cells) were recorded.
21. The firing fields of a subset of MEC cells had the stripe-like appearance of boundary vector cells, but only 6 of 19 fired maximally at the border. A field size criterion (>625 cm^2) rather than the border score was thus used to include these cells (see also fig. S8).
22. N. Burgess, J. O'Keefe, *Hippocampus* **6**, 749 (1996).
23. C. Lever, S. Burton, A. Jeewajee, J. O'Keefe, N. Burgess, *J. Neurosci.* **29**, 9771 (2009).
24. T. Solstad, C. N. Boccara, E. Kropff, M. B. Moser, E. I. Moser, *Science* **322**, 1865 (2008).
25. C. T. Dickson, J. Magistretti, M. Shalinsky, B. Hamam, A. Alonso, *Ann. N. Y. Acad. Sci.* **911**, 127 (2000).
26. S. J. Mizumori, B. L. McNaughton, C. A. Barnes, K. B. Fox, *J. Neurosci.* **9**, 3915 (1989).
27. E. Brazhnik, R. Borgnis, R. U. Muller, S. E. Fox, *J. Neurosci.* **24**, 9313 (2004).
28. E. A. Zilli, M. E. Hasselmo, *J. Neurosci.* **30**, 13850 (2010).
29. M. P. Brandon *et al.*, *Science* **332**, 595 (2011).
30. T. Hafting, M. Fyhn, T. Bonnevie, M. B. Moser, E. I. Moser, *Nature* **453**, 1248 (2008).

31. The authors thank T. Solstad and E. Mankin for Matlab scripts and M. Hasselmo, L. Squire, and M. Scanziani for comments and discussions. Supported by the Walter F. Heiligenberg Professorship, NSF/NIH/Bundesministerium für Bildung und Forschung grant 1010463, Ellison Medical Foundation grant AG-NS-0724-10, the Alfred P. Sloan Foundation, and Alzheimer's Association grant NIRG-09-133414.

Supporting Online Material

www.sciencemag.org/cgi/content/full/332/6029/592/DC1
Materials and Methods
Figs. S1 to S11
Table S1
References

14 December 2010; accepted 24 March 2011
10.1126/science.1201685

Reduction of Theta Rhythm Dissociates Grid Cell Spatial Periodicity from Directional Tuning

Mark P. Brandon,* Andrew R. Bogaard, Christopher P. Libby, Michael A. Connerney, Kishan Gupta, Michael E. Hasselmo*

Grid cells recorded in the medial entorhinal cortex of freely moving rats exhibit firing at regular spatial locations and temporal modulation with theta rhythm oscillations (4 to 11 hertz). We analyzed grid cell spatial coding during reduction of network theta rhythm oscillations caused by medial septum (MS) inactivation with muscimol. During MS inactivation, grid cells lost their spatial periodicity, whereas head-direction cells maintained their selectivity. Conjunctive grid–by–head-direction cells lost grid cell spatial periodicity but retained head-direction specificity. All cells showed reduced rhythmicity in autocorrelations and cross-correlations. This supports the hypothesis that spatial coding by grid cells requires theta oscillations, and dissociates the mechanisms underlying the generation of entorhinal grid cell periodicity and head-direction selectivity.

The role of oscillations in neural coding is controversial. Theta frequency oscillations (4 to 11 Hz) play an important role in memory behavior (*1*–*4*) and code spatial location by the precession of spike timing relative to theta oscillations (theta phase precession) in the hippocampus (*5*, *6*) and medial entorhinal cortex (MEC) (*7*). However, disagreement remains about whether theta oscillations are critical to spatial coding by neurons. Grid cells (*8*, *9*) in the MEC provide a powerful example for testing the theoretical role of oscillations in neural coding. Some computational models of grid cells use network theta rhythm oscillations to generate grid cell spatial periodicity (*10*, *11*). These models simulate the phase of spike timing in grid cells (*7*)

Center for Memory and Brain, Department of Psychology, Graduate Program for Neuroscience, Boston University, 2 Cummington Street, Boston, MA 02215, USA.

*To whom correspondence should be addressed. E-mail: hasselmo@bu.edu (M.E.H.); markpb68@bu.edu (M.P.B.)

and have successfully predicted that the spatial scale of grid cell firing correlates with measures of intrinsic rhythmicity (*12*, *13*). Recent models also show the potential role of theta oscillations for updating position in attractor dynamic models of grid cells (*14*). In rats, we tested the role of theta rhythm oscillations in the spatial coding of grid cells by testing the spatial periodicity of grid cells during pharmacological disruption of theta rhythm oscillations.

Lesions or inactivation of the medial septum (MS) in rats cause a disruption of theta oscillations in the entorhinal-hippocampal system (*2*, *4*, *15*, *16*) and cause spatial memory impairments (*1*–*4*, *17*, *18*). We performed microinfusions of muscimol to pharmacologically inactivate the MS bilaterally (*1*, *17*). Simultaneously, we used tetrodes in the MEC to monitor the spiking activity of grid cells, head-direction cells, and conjunctive grid–by–head-direction cells.

After infusions of muscimol into the MS (Fig. 1A, left), recordings in the MEC (Fig. 1A, right) demonstrated a clear decrease in the power of theta oscillations in the MEC local field potential (Fig. 1B) and a strong reduction in the spatial periodicity of grid cells (Figs. 1, C and D, and 2A and fig. S3). Recovery of theta rhythm and spatial periodicity occurred in recordings 3 to 6 hours and 24 hours after the infusion. The "gridness" (hexagonal regularity of firing) score measured before the MS inactivation showed a significant decrease after the inactivation (n = 29 cells; baseline: mean ± standard error: 0.64 ± 0.05 gridness score; inactivation: −0.27 ± 0.06 gridness score, P < 0.001) (Fig. 3A) that recovered at 3 to 6 hours and 24 hours (3 to 6 hours: n = 26, 0.35 ± 0.10 gridness score; 24 hours: n = 21, 0.46 ± 0.09 gridness score). Because the firing rates of grid cells were also reduced (n = 29; baseline: 1.88 ± 0.20 Hz; inactivation: 1.17 ± 0.21 Hz, P < 0.001), we subsampled the spiking of the baseline recordings before infusion to match the same overall firing rate after infusion to confirm that the reduction of gridness still appeared when compared to subsampled data (n = 29; subsampled: 0.58 ± 0.05 gridness score; inactivation: −0.27 ± 0.06 gridness score, P < 0.001) (column 2 in Fig. 1, C and D, and fig. S3). There were no differences in running speeds between the baseline, MS inactivation, 3- to 6-hour, or 24-hour recovery periods (Fig. 4C and fig. S8). Control infusions of phosphate-buffered saline (PBS) into the MS did not alter theta oscillations or the grid cell spiking patterns in the MEC (Fig. 1E and fig. S7).

Many neurons in the MEC are conjunctive grid–by–head-direction cells (*19*, *20*), head-direction cells (*19*, *21*), or cells showing spatial selectivity without grid cell periodicity, such as border cells (*22*, *23*). We observed a dissociation in the effect of MS inactivation on the spatial periodicity and head-direction specificity of entorhinal neurons. After muscimol infusion, conjunctive grid–by–head-direction cells fired with reduced spatial periodicity (Fig. 2A

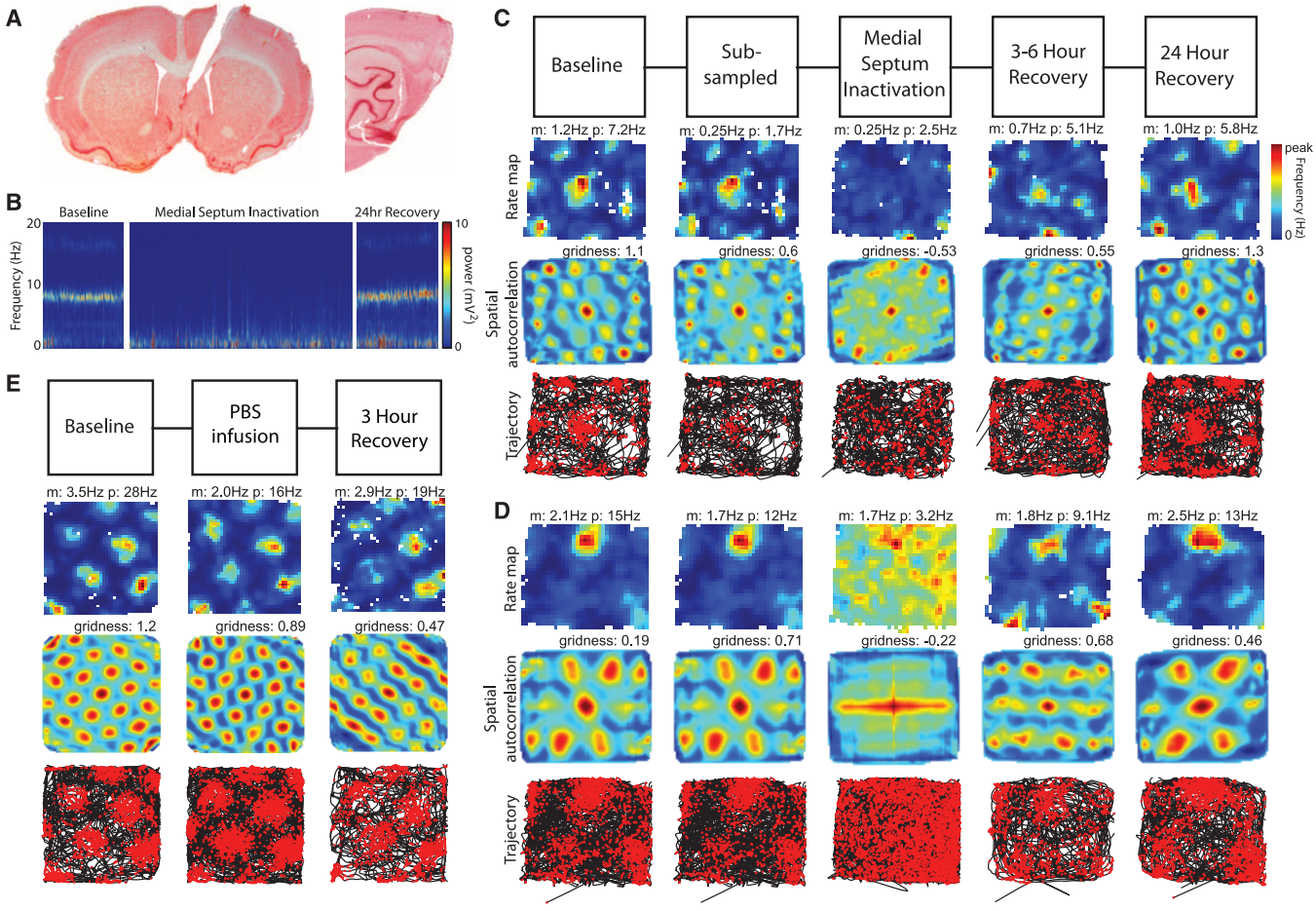

Fig. 1. Loss of grid cell spatial periodicity during reduced theta rhythm oscillations. (**A**) (Left) Muscimol infusions were delivered via a cannula in the MS. (Right) Tetrode tracks show the location of recording in the MEC. (**B**) Spectrogram of MEC local field potential showing loss of pre-infusion theta peak after infusion. (**C**) Column 1: Grid cell firing before infusion (Baseline). m, mean rate; p, peak rate. Column 2: Subsampling of pre-infusion firing rate to match rate 15 to 75 min after infusion. Column 3: Grid cell firing 15 to 75 min after muscimol infusion (Medial Septum Inactivation) demonstrating loss of grid cell spatial periodicity during reduced theta. Columns 4 and 5: Recovery 3 to 6 hours (3-6 Hour Recovery) and 24 hours (24 Hour Recovery) after infusion. Row 1, firing rate maps; row 2, autocorrelation maps; row 3, animal trajectory with spikes (red dots). (**D**) Example of another grid cell before and after infusion. (**E**) Example of grid cell firing before and after control infusion of PBS.

and fig. S3) but retained their directional preference, ϕ [n = 8, 1.72 ± 1.15 |Δϕ| degrees, not significant (n.s.)] (Figs. 2A and 3B and fig. S3). After infusion, head-direction cells retained their directionality (n = 11; baseline: 37.89 ± 8.9 Watson U^2 statistic; inactivation: 39.55 ± 14.54 Watson U^2 statistic, n.s.; 24.64 ± 9.17 |Δϕ| degrees, n.s.) (Figs. 2B and 3B and fig. S4) and as a population retained their firing rates (n = 11; baseline: 2.7 ± 0.72 Hz; inactivation: 1.9 ± 0.65 Hz, n.s.) (Fig. 3A). Cells with positive gridness scores showed a reduction of spatial information (grid cells: n = 29; baseline: 1.08 ± 0.07 bits per spike; inactivation: 0.56 ± 0.05 bits per spike, P < 0.001) (Fig. 3A). Cells with negative gridness scores but high spatial information also showed a reduction of spatial information (spatially modulated non-grid cells: n = 9; baseline: 1.3 ± 0.15 bits per spike; inactivation: 0.70 ± 0.10 bits per spike, P < 0.01) (Fig. 3A and fig. S5).

The slow onset and long half-life that are characteristic of muscimol effects (*1*, *17*) permitted us to quantify the relationship between theta power and grid cell spiking. Using 10-min sliding window calculations, we found a clear similarity in the time course between theta power and gridness (Fig. 3D) and a consistent relationship between the power of theta and the gridness score (Fig. 3C). Could a drift in spatial phase or orientation explain the loss of the grid pattern after infusion? Across all of our recording sessions, large gridness scores did not appear during periods of low theta index (Fig. 3, C and D). A drifting grid cell representation would usually maintain the relative spike timing between simultaneously recorded grid cells. When multiple grid cells were recorded, they often showed rhythmic peaks in their spike time cross-correlations that were reduced or eliminated during MS inactivation (Fig. 4B), as shown by the reduction of power in the theta rhythm in cross-correlations, suggesting a reduction of temporal consistency. During MS inactivation, the cross-correlation plots reveal a reduction in percentage of theta rhythmic cells (baseline: 53%, inactivation: 23%, n = 350) and theta power ratio (baseline: 3.4 ± 0.01, inactivation: 0.23 ± 0.01, n = 187, P < 0.001). Autocorrelation plots show a reduced percentage of theta rhythmic cells (baseline: 38%, inactivation: 15%, n = 78) and autocorrelation theta power ratio (baseline: 4.1 ± 0.35, inactivation: 1.37 ± 0.21, n = 30, P < 0.001). A decrease in the frequency of remaining theta rhythmic cells appeared in both cross-correlations (n = 62; baseline: 6.83 ± 0.02, inactivation: 6.34 ± 0.06, P < 0.001) and autocorrelations (n = 10; baseline: 7.10 ± 0.08, inactivation: 6.66 ± 0.27) (Fig. 4, B and D). The frequency increase at 3 to 6 hours (Fig. 4D) may arise from rebound of currents after inactivation. Some autocorrelation plots also exhibited theta cycle skipping (*24*) during control conditions (Fig. 4B), yet lost this attribute during MS inactivation (baseline: n = 30, 60% of theta rhythmic cells; inactivation: n = 13, 0% of theta rhythmic cells; theta skipping index, n = 12, baseline: 0.08 ± 0.03, inactivation: −0.12 ± 0.01, P < 0.001).

These results are complementary to the results obtained independently by Koenig *et al.* (*25*). The use of muscimol here demonstrates the correlated reduction of theta power and gridness score over a long time course, and the use of lidocaine in the companion paper shows the relationship over a faster time course. The recording in deeper layers of the entorhinal cortex here demonstrates the sparing of head-direction selectivity in conjunctive cells and in pure head-direction cells, and the companion paper shows the sparing of hippocampal place cell specificity, consistent with previous studies (*26*). Our data show a reduction of rhythmicity in temporal cross-correlations between

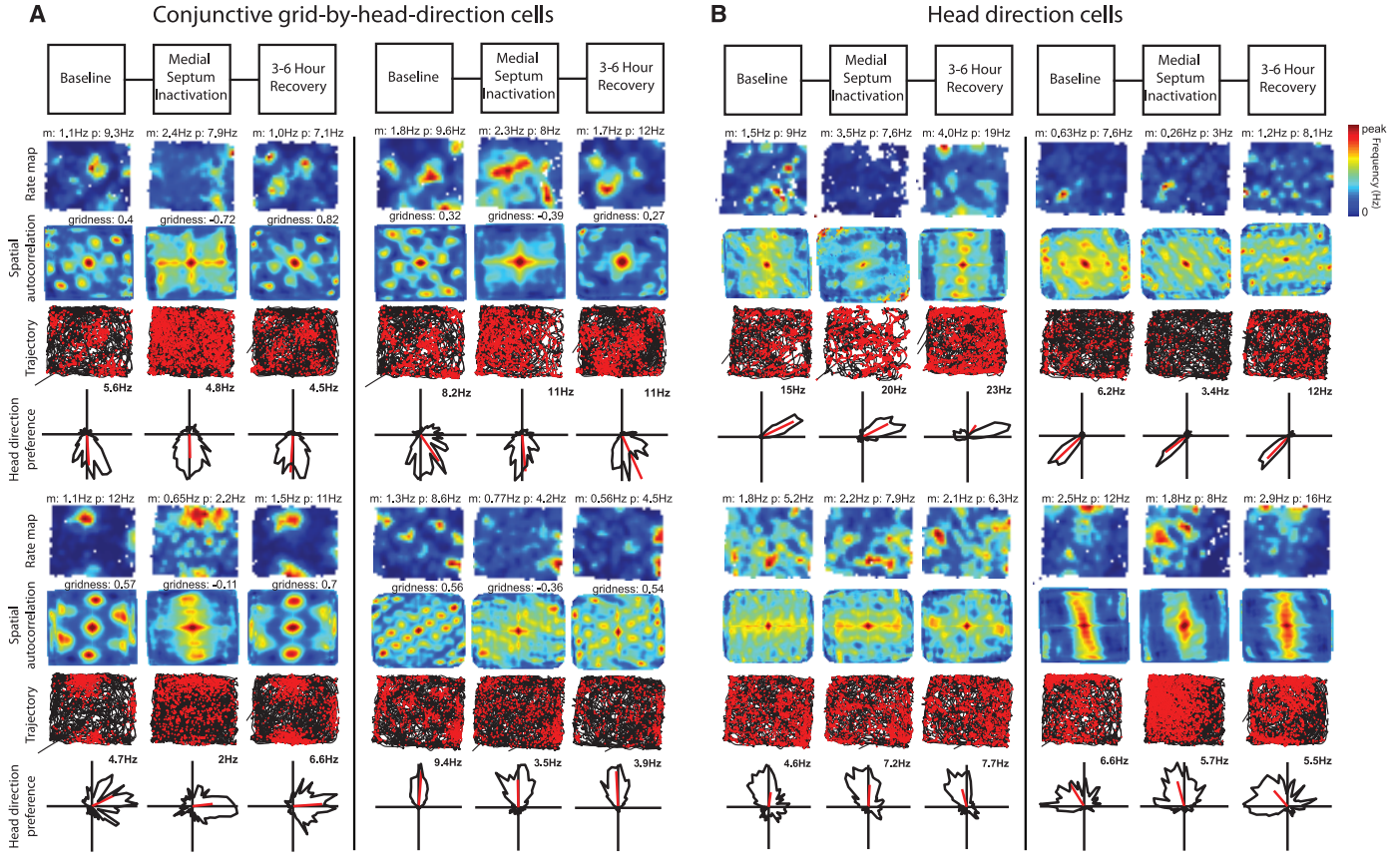

Fig. 2. Head-direction selectivity is spared. (**A**) Examples of four conjunctive grid–by–head-direction cells. The selectivity for head direction observed before infusion (Baseline) remains during MS inactivation despite the loss of grid cell spatial periodicity in the spatial maps. (**B**) Four head-direction–selective cells without spatial periodicity before infusion (Baseline) maintain head-direction preference during MS inactivation. Overall firing rates are not reduced in either cell type.

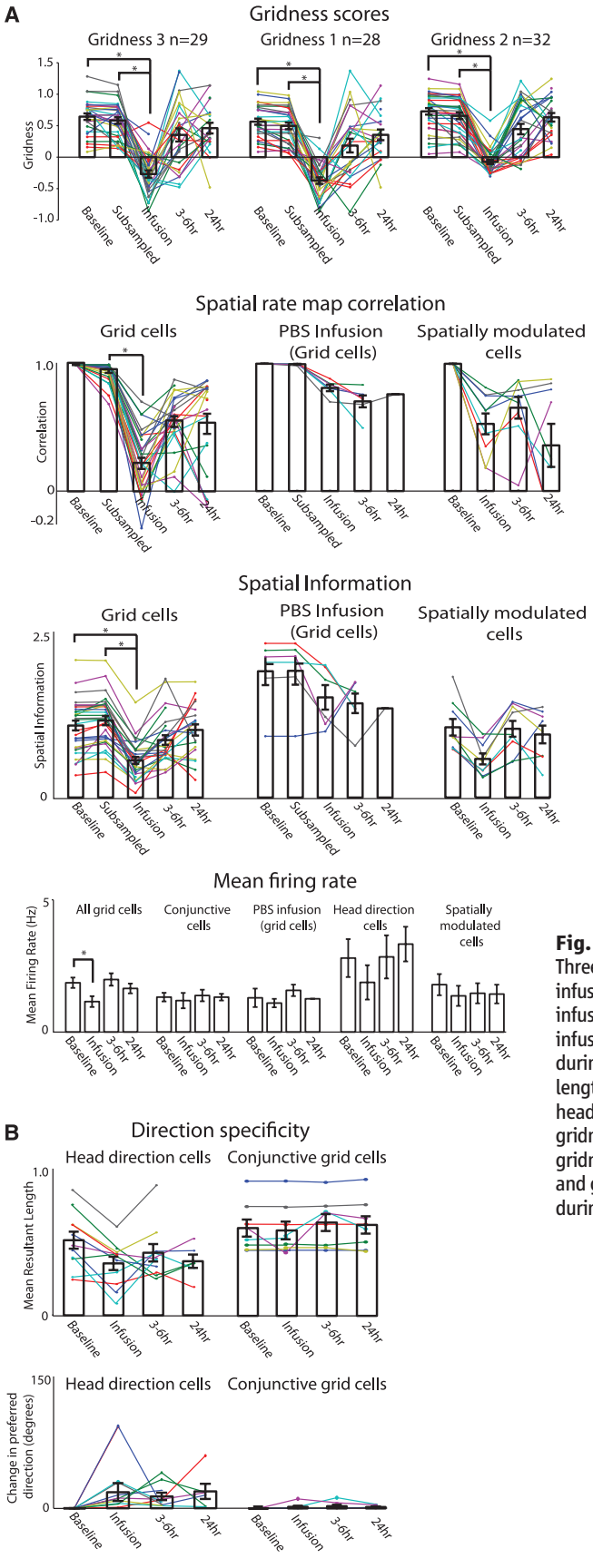

Fig. 3. Statistics for grid cells, head-direction cells, and spatially modulated cells. (**A**) (Top) Three gridness measures show a sharp reduction in gridness 15 to 75 min after muscimol infusion (MS Inactivation), with recovery at 3 to 6 hours (3-6hr) and 24 hours (24hr) after infusion. (Middle) Spatial map correlations and spatial information for grid cells, PBS infusions, and spatially modulated cells for each period. (Bottom) Average firing rate during each period for all cell types. (**B**) Head-direction cell statistics. Mean resultant length and change in head-direction preference angle from baseline (in degrees) for all head-direction cells and conjunctive cells during each period are shown. (**C**) Average gridness score at different levels of theta power. There is a consistent relationship between gridness and theta power. (**D**) Time course of the effect of MS inactivation on theta power and gridness score computed in a sliding 10-min window at 1-min intervals for each period during the experiment, showing similar reduction and recovery.

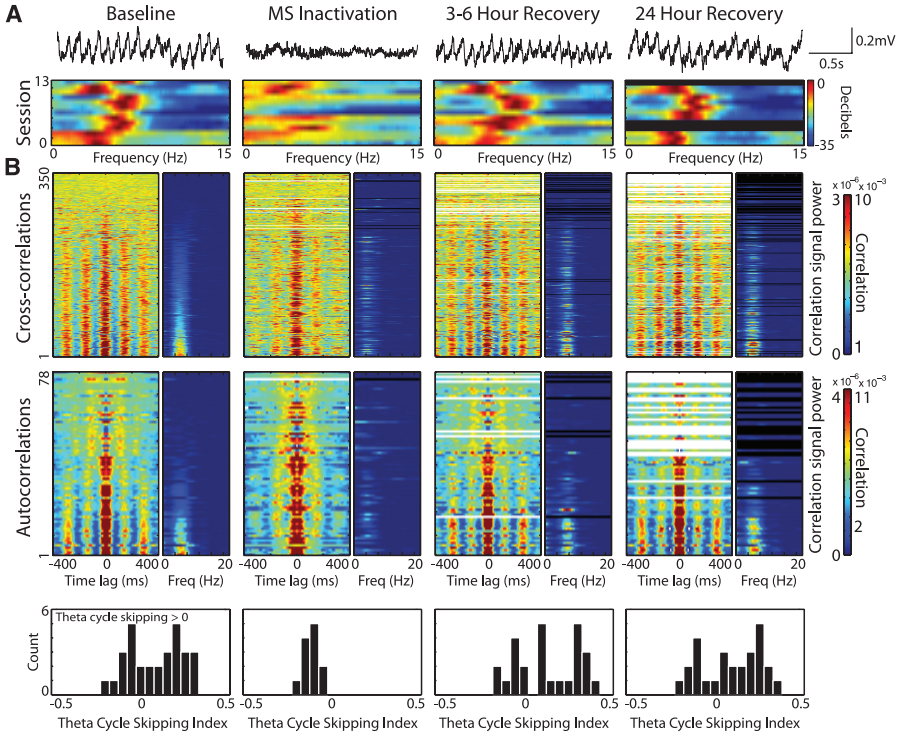

Fig. 4. Temporal coordination of local field potential and spike timing disrupted during MS inactivation. (**A**) (Top) Raw electroencephalogram shows reduction of theta rhythm during MS inactivation. (Bottom) Power spectrum of MEC local field potential for 13 sessions during periods before (Baseline), 15 to 75 min after (MS inactivation), 3 to 6 hours after, and 24 hours after infusion. (**B**) (Top) For each period, the left graph shows temporal cross-correlations ordered by the ratio $Power_{theta}/Power_{signal}$. The right graph shows respective power spectra. Reduction in theta power after infusion in cross-correlations suggests loss of timing relationships between cells. There is a decrease in frequency during MS inactivation. (Middle) Temporal autocorrelations of spiking show reduction in theta power and frequency during MS inactivation. (Bottom) Theta cycle skipping index for all theta rhythmic neurons for each period. An index greater than zero indicates that the second peak in autocorrelation is larger than the first peak. Theta skipping is lost during MS inactivation. (**C**) (Left) Theta power (the ratio between power in the theta and delta bands) decreases during MS inactivation. (Right) Average running speed for each period did not change during infusion. (**D**) (Top) Cross-correlation and autocorrelation frequency for each cell pair or cell during each period shows a reduction in frequency during MS inactivation and an increase 3 to 6 hours after infusion. (Bottom) Percentage of cells showing theta rhythmicity in cross-correlations and autocorrelations during each period. There is a reduction of theta rhythmic cells and cell pairs during MS inactivation.

simultaneously recorded neurons during MS inactivation. The combined data suggest that grid cell spatial periodicity is not essential for place cell responses in familiar environments, which is consistent with studies suggesting that the development of place cell responses does not depend on the development of grid cell responses (*27*, *28*).

These data support the hypothesized role of theta rhythm oscillations in the generation of grid cell spatial periodicity (*10*–*12*) or at least a role of MS input. The loss of grid cell spatial periodicity could contribute to the spatial memory impairments caused by lesions (*3*, *4*, *18*, *29*) or inactivation (*1*, *2*, *17*) of the MS. These data support a role of neuronal oscillations in the coding of spatial information.

References and Notes

1. B. Givens, D. S. Olton, *J. Neurosci.* **14**, 3578 (1994).
2. S. J. Mizumori, G. M. Perez, M. C. Alvarado, C. A. Barnes, B. L. McNaughton, *Brain Res.* **528**, 12 (1990).
3. J. Winson, *Science* **201**, 160 (1978).
4. S. J. Mitchell, J. N. Rawlins, O. Steward, D. S. Olton, *J. Neurosci.* **2**, 292 (1982).
5. J. O'Keefe, M. L. Recce, *Hippocampus* **3**, 317 (1993).
6. W. E. Skaggs, B. L. McNaughton, M. A. Wilson, C. A. Barnes, *Hippocampus* **6**, 149 (1996).
7. T. Hafting, M. Fyhn, T. Bonnevie, M. B. Moser, E. I. Moser, *Nature* **453**, 1248 (2008).
8. E. I. Moser, M. B. Moser, *Hippocampus* **18**, 1142 (2008).
9. M. Fyhn, S. Molden, M. P. Witter, E. I. Moser, M. B. Moser, *Science* **305**, 1258 (2004).
10. N. Burgess, C. Barry, J. O'Keefe, *Hippocampus* **17**, 801 (2007).
11. J. O'Keefe, N. Burgess, *Hippocampus* **15**, 853 (2005).
12. L. M. Giocomo, E. A. Zilli, E. Fransén, M. E. Hasselmo, *Science* **315**, 1719 (2007).
13. A. Jeewajee, C. Barry, J. O'Keefe, N. Burgess, *Hippocampus* **18**, 1175 (2008).
14. Z. Navratilova, L. M. Giocomo, J. M. Fellous, M. E. Hasselmo, B. L. McNaughton, *Hippocampus*, 10.102/hipo.20939 (2011).
15. J. N. Rawlins, J. Feldon, J. A. Gray, *Exp. Brain Res.* **37**, 49 (1979).
16. K. J. Jeffery, J. G. Donnett, J. O'Keefe, *Neuroreport* **6**, 2166 (1995).
17. J. J. Chrobak, R. W. Stackman, T. J. Walsh, *Behav. Neural Biol.* **52**, 357 (1989).
18. M. M. Martin, K. L. Horn, K. J. Kusman, D. G. Wallace, *Physiol. Behav.* **90**, 412 (2007).
19. F. Sargolini *et al.*, *Science* **312**, 758 (2006).
20. C. N. Boccara *et al.*, *Nat. Neurosci.* **13**, 987 (2010).
21. J. S. Taube, R. U. Muller, J. B. Ranck Jr., *J. Neurosci.* **10**, 420 (1990).
22. C. Lever, S. Burton, A. Jeewajee, J. O'Keefe, N. Burgess, *J. Neurosci.* **29**, 9771 (2009).
23. T. Solstad, C. N. Boccara, E. Kropff, M. B. Moser, E. I. Moser, *Science* **322**, 1865 (2008).
24. S. S. Deshmukh, D. Yoganarasimha, H. Voicu, J. J. Knierim, *J. Neurophysiol.* **104**, 994 (2010).
25. J. Koenig, A. N. Linder, J. K. Leutgeb, S. Leutgeb, *Science* **332**, 592 (2011).
26. S. J. Mizumori, B. L. McNaughton, C. A. Barnes, K. B. Fox, *J. Neurosci.* **9**, 3915 (1989).
27. R. F. Langston *et al.*, *Science* **328**, 1576 (2010).
28. T. J. Wills, F. Cacucci, N. Burgess, J. O'Keefe, *Science* **328**, 1573 (2010).
29. K. C. Pang, R. Nocera, *Behav. Neurosci.* **113**, 265 (1999).

30. Thanks to C. Stern, S. Leutgeb, H. Eichenbaum, N. Schultheiss, E. Newman, C. Monaghan, J. Climer, and E. Zilli for advice and comments and to T. Ware for technical assistance. The research was supported by National Institute of Mental Health grants R01 MH60013 and MH61492 and Office of Naval Research Multidisciplinary University Research Initiative grant N00014-10-1-0936.

Supporting Online Material

www.sciencemag.org/cgi/content/full/332/6029/595/DC1
Materials and Methods
SOM Text
Figs. S1 to S8
References

14 December 2010; accepted 24 March 2011
10.1126/science.1201652